A potential strategy to treat liver fibrosis

Gonzalo Lázaro, Teresa

Chapter 6

Local inhibition of liver fibrosis by specific delivery of a PDGF kinase inhibitor to hepatic stellate cells

Submitted for publication.

[1,]Teresa Gonzalo, [1]Leonie Beljaars, [1]Marja van de Bovenkamp, [1]Anne-Miek van Loenen, [1]Catharina Reker-Smit, [1]Dirk K.F. Meijer, [2]Marie Lacombe, [2]Frank Opdam, [3]György Kéri, [3]László Orfi, [1]Klaas Poelstra, [1,4]Robbert J Kok.

[1]Department of Pharmacokinetics and Drug Delivery, Groningen University Institute for Drug Exploration, University of Groningen, The Netherlands;

[2]Kreatech Biotechnology B.V., Amsterdam;

[3]Department of Medical and Pharmaceutical Chemistry, Semmelweis University, Budapest, Hungary;

[4]Department of Pharmaceutics, Utrecht University, The Netherlands.

Abstract

Liver fibrosis is characterized by an excessive proliferation and activation of Hepatic Stellate Cells (HSC). Platelet-derived growth factor (PDGF-BB) is the most potent mitogen for HSC and inhibition of PDGF signalling via specific delivery of a PDGF kinase inhibitor to HSC might therefore be an attractive strategy to counteract the progression of liver fibrosis. The HSC-selective carrier M6PHSA was equipped with a PDGF receptor tyrosine kinase inhibitor (PTKI, an imatinib derivative) by means of a novel platinum-based linker (ULS™).

Culture-activated rat HSC and precision-cut liver slices from fibrotic rats were incubated with PTKI-M6PHSA and fibrosis markers were evaluated by quantitative RT-PCR. The gene expression of α-smooth muscle actin and α1-(I)-procollagen were reduced by 50% in both *in vitro* systems after treatment with PTKI-M6PHSA (0.1 mg/ml, corresponding to 10μM of PTKI) and free PTKI showed similar effects.

Next, we examined the homing and antifibrotic effects of PTKI-M6PHSA in bile duct ligated (BDL) rats. Male Wistar rats at day 10 after BDL were injected intravenously with a single dose of 3.3 mg/kg of PTKI-M6PHSA and compared with non-treated BDL rats. PTKI-M6PHSA was detected in the liver 2h after administration in a non-parenchymal distribution pattern. The antifibrotic effects of PTKI-M6PHSA were analysed by Sirius Red and α-smooth muscle actin stainings. Both parameters were reduced 24h and 48h after the single dose of PTKI-M6PHSA ($p<0.01$, $p<0.05$. resp), in comparison with non-treated rats. We subsequently conducted a multiple dose study administering PTKI-M6PHSA to BDL rats and untargeted PTKI, where we found no effect of either treatment.

In summary, PTKI-M6PHSA showed an antifibrogenic effect in cultured HSC and fibrotic liver slices. This effect was also demonstrated *in vivo* after direct targeting of the PDGFR kinase inhibitor to activated HSC during liver fibrosis after single administration. Upon longer treatment however, PDGF kinase inhibition can not block the fibrotic

process. We therefore conclude that delivery of a PDGF-kinase inhibitor to HSC is a promising technology to attenuate liver fibrogenesis, although other activating pathways may need to be inhibited in parallel.

A

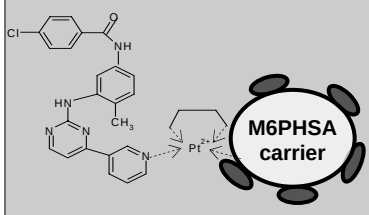

PTKI-M6PHSA

Theoretical synthesis ratio PTKI-ULS: protein	Coupling ratio PTKI : protein¶	Yield of synthesis#
10:1	8 : 1 (±1.9)	84%

B

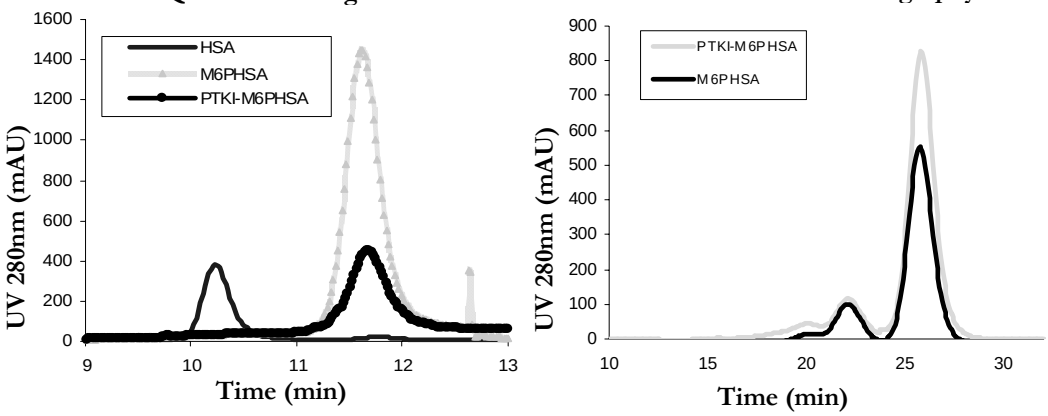

Figure 1. Characteristics of PTKI-M6PHSA drug targeting conjugate.

A. Synthesis of PTKI-M6PHSA. PTKI was conjugated via the platinum based linker ULS to the stellate cell selective carrier M6PHSA. Coordination bonds between drug-linker and linker-carrier are depicted as dotted lines. ¶ PTKI/M6PHSA coupling ratio was determined by HPLC after competitive displacement of the drug with potassium thiocyanate (KSCN) at 80°C for 24h. # Based in the BCA assay or protein concentration. Values obtained from three independent PTKI-M6PHSA synthesized conjugates. B. MonoQ anion exchange chromatography confirmed that the charge of the protein was not affected. Size exclusion chromatography showed the monomeric composition of PTKI-M6PHSA. M6PHSA: mannose-6-phosphate modified human serum albumin; ULS: Universal Linkage System.

Introduction

Liver fibrosis is a proliferative disease that may be initiated by a variety of factors including chronic hepatitis, virus infections, alcohol drinking, and drug abuse. It has been extensively documented that activated hepatic stellate cells (HSC) play a fundamental role in the development of liver fibrosis (1;2). During liver fibrosis, activated HSC proliferate and deposit extracellular matrix proteins, a process that is driven by an array of cytokines and growth factors. Among these, platelet-derived growth factor (PDGF-BB) has been identified as the most potent mitogen for HSC (3). Activated HSC produce PDGF (4) and PDGFR-β receptors are highly upregulated on the cell surface of hepatic stellate cells during fibrosis (5-7).

Imatinib (STI 571, Gleevec) is employed in the treatment of chronic myelogenous leukaemia (CML) and gastrointestinal stromal tumors (GISTs) (8). It inhibits several tyrosine kinases that are mutated during cancer development. In addition, imitanib is a potent inhibitor of PDGF-B kinase. Consequently, imatinib has been tested for its antifibrotic effect in cultured HSC (9) and has recently been evaluated in different animal models of liver fibrosis (10-13). The fundamental role that PDGF signalling appears to play in liver fibrogenesis has made it an attractive therapeutic target for the treatment of liver fibrosis (14).

In the present study, we have investigated whether the antifibrotic effects of a PDGF tyrosine kinase inhibitor (PTKI), a drug structurally associated to imatinib (15), can be enhanced by local delivery to HSC in the fibrotic liver. PDGF tyrosine kinase activity plays a role in many more processes than HSC proliferation, so it is reasonable to expect side effects of its inhibition. Drug targeting strategy can improve the effect of the drug by increasing local concentrations at the target site and by providing slow local drug release. It will also prevent side effects in other tissue or organs (16).

To effectuate local delivery and effects within HSC in the liver, we have developed a new drug targeting construct, PTKI-M6PHSA, in which PTKI is coupled to the HSC-directed carrier protein mannose-6-phosphate-human serum albumin (M6PHSA). M6PHSA is a

well-established carrier that binds to the M6P/IGFII receptor on HSC and accumulates rapidly and extensively in the liver of fibrotic rats (17). To conjugate PTKI to M6PHSA, we have employed a novel type of platinum linker chemistry called ULS™ (Universal Linker System)(18). ULS allows stable coupling of drug molecules to proteins based on the formation of a platinum-ligand coordination bond (19). Application of this novel linker technology was essential since it appears to be straightforward and reliable for linking PTKI molecules to the carrier, allowing high synthesis yields in a relatively simple approach. Second, the resulting PTKI-ULS-M6PHSA conjugates display a unique behavior of slow release of drug molecules during a period of days within the designated target cells.

In the present study, we describe the development of PTKI-M6PHSA and its impact on liver fibrogenesis *in vitro* and *in vivo*. Culture of HSC and fibrotic liver slices were employed as *in vitro* systems to prove the antifibrotic effect of PTKI-M6PHSA. In addition, PTKI-M6PHSA was tested in a model of liver fibrosis to study the distribution and effects on the development of liver fibrosis.

	BDL day 10 control saline	BDL day 11 control saline	BDL day 12 control saline	BDL day 10 +PTKI-M6PHSA	BDL day 11 +PTKI-M6PHSA	BDL day 12 +PTKI-M6PHSA
Number of rats	5	5	5	3	5	5
Body weight (g)	250.2 ± 46.7	311.2 ± 14.7	273.4 ± 16.4	280.7 ± 10.1	301.4 ± 14.1	306.4 ± 13.5
Liver/body ratio (g/g)	0.055 ± 0.009	0.062 ± 0.007	0.065 ± 0.004	0.061 ± 0.002	0.060 ± 0.006	0.065 ± 0.009
Dose	Saline	Saline	Saline	3.3mg/kg	3.3mg/kg	3.3mg/kg
Bilirubin (umol/l)	183.7 ± 35.8	178.0 ± 48.2	228.5 ± 18.7	252.3 ± 55.9	136.0 ± 10.0	183.5 ± 27.9
ALT (U/l)	86.3 ±30.9	79.8 ±46.1	79.3 ±11.2	96.5 ± 4.9	72.7 ±10.6	81.0 ±17.0
Alkaline Phosphatase (U/l)	391.2 ±46.4	476.0 ±162.6	358.3 ±234.1	458.0 ±11.2	426.0±101.3	511.3±121.4

Table 1. Dose regimens, animal data and biochemical parameters from PTKI-M6PHSA single injection study*. Data are shown as mean ± SD. BDL, bile duct ligated animals; ALT, alanine aminotransferase.*

Materials and methods

Materials

The Protein Tyrosine Kinase Inhibitor (PTKI, 4-Chloro-N-[4-methyl-3-(4-pyridin-3-yl-pyrimidin-2-ylamino)-phenyl]-benzamide) was kindly provided by György Kéri (Vichem Chemie Research Ltd., Budapest, Hungary). M6PHSA was prepared as described previously (19). Cis-[Pt(ethylenediamine)nitrate-chloride] (cisULS) was prepared as previously described (19).

Synthesis of PTKI-ULS-M6PHSA

PTKI-ULS was synthesized and purified by Kreatech Biotechnology (Amsterdam, The Netherlands). In brief, PTKI (7.2 μmol, 3 mg; 10 mg/ml in DMF) was mixed with an equimolar amount of cisULS (7.2 μmol, 2.4 mg; 20 mM in DMF). The reaction mixture was heated at 37°C for 24h after which consumption of the starting material was monitored by analytical HPLC. An additional amount of cisULS was added (0.5 equivalent, 3.6 μmol) and the reaction was continued for 48h at 37°C. The crude mixture was concentrated under reduced pressure and dissolved in methanol (600 μl). The crude product was purified by preparative HPLC and the collected peaks of the main product were taken to dryness under reduced pressure. The resulting white solid was treated with water to remove anorganic salts and dried. Yield: 0.9 mg (20%). Mass spectrometry analysis confirmed the presence of the 1:1 PTKI-ULS species.

^{1}H NMR of **PTKI** (CD_3OD): δ_H 2.33 (s, 3H, CH_3), 7.26 (d, J = 8.28 Hz, 1H, CCH_3C**H**), 7.37 (m, 2H, C**H**C**l**), 7.52 (m, 3H, N(C**H)$_2$CC**C**C**H**), 7.93 (d, J = 8.60 Hz, 2H, C**H**CHCl), 8.22 (s, 1H, NHCC**H**C), 8.47 (d, J = 5.23 Hz, 1H, C**HNC**NH), 8.64 (m, 2H, C**H**$(CH)_2$C and CHC**H**CNH), 9.29 (s, 1H, NCHC) ppm.

^{1}H NMR of **PTKI**-ULS (CD_3OD): δ_H 2.27 (m, 3H, CH_3), 2.66 (m, 2H, CH_2), 2.74 (m, 2H, CH_2), 7.15 (m, 3H, C**H**CCH_3 and C**H**C**l**), 7.47 (m, 3H, N(C**H)$_2$CC**C**C**H**), 7.84 (d, J = 5.23 Hz, 1H, CHC**H**CNH), 7.89 (m, 2 H, C**H**CHCl), 8.39 (d, J = 3.95 Hz, 1H, C**HNC**NH) ppm.

Mass spectrometry of PTKI-ULS (ESI+): calculated mass: 705 (m/z); detected masses: 706 $[M]^+$, 688 $[M\text{-}Cl^-+OH^-]^+$, 670 $[M\text{-}Cl^-\text{-}H^+]^+$, 669 $[M\text{-}Cl^-\text{-}H^+]^+$, 651 $[M\text{-}Cl^-\text{-}Cl^-+OH^-+H]^+$.

HPLC analysis: Separations were performed on a Luna2 C18 column that was maintained at 40°C. The mobile phase consisted of a binary solvent system of triethylammonium acetate (100mM pH 5.0):acetonitrile 90:10 (solvent A) and triethylammonium acetate (100mM pH 5.0):acetonitrile 70:30 (solvent B). The column was eluted at a flow rate of 1.1 mL/min. Compounds were eluted at a stepwise gradient (0%B from 0-4 min; 0-46%B from 4-17 min; 46-100%B from 17-19 min; 100%B from 19-25 min; 100-0%B from 25-27 min; 0%B from 27-34 min). PTKI eluted at 21.2 min (60.8%B) and PTKI-ULS eluted at 11.5 min (26.5%B).

PTKI-ULS was conjugated to M6PHSA according to a general protocol that has been described elsewhere for the synthesis of Pentoxifylline-ULS-M6PHSA (19). Briefly, PTKI-ULS (143 nmol, 1.6 mg that was dissolved in DMF/H2O at 6.7 mg/ml) was added in 10-fold molar excess to M6PHSA (14.3 nmol, 10 mg, dissolved in 1 ml of 20 mM tricine/$NaNO_3$ buffer pH 8.3). The pH was checked and adjusted to pH 8 if necessary. The mixture was incubated overnight at 37°C, and dialysed against PBS at 4°C. The final product was sterilized by filtration via a 0.2 μm filter and stored at -20°C. Protein content was assessed by the BCA assay (Pierce, Rockford, IL, USA). PTKI-M6PHSA and M6PHSA were analyzed by size-exclusion chromatography and anion exchange chromatography as described before (17) to verify that coupling of PTKI-ULS did not alter the properties of the M6PHSA protein. The amount of PTKI coupled to M6PHSA was analyzed by isocratic HPLC after competitive displacement of the drug by overnight incubation at 80°C with excess of potassium thiocyanate (KSCN, 0.5M in PBS). Elutions were performed on a Waters system (Waters, Milford, MA, USA) equipped with a 5 μm Hypersil BDS C8 column (250x4.6 mm, Thermoquest Runcorn, UK), a thermostated column oven operated at 40°C and an UV detector operated at 269 nm. The mobile phase consisted of acetonitrile/water/trifluoracetic acid (40/60/0.1, pH 2) at a flow rate of 1.0 ml/min with a sensitivity of 0.01. Retention times: PTKI: 7 min; PTKI-ULS: 5 min.

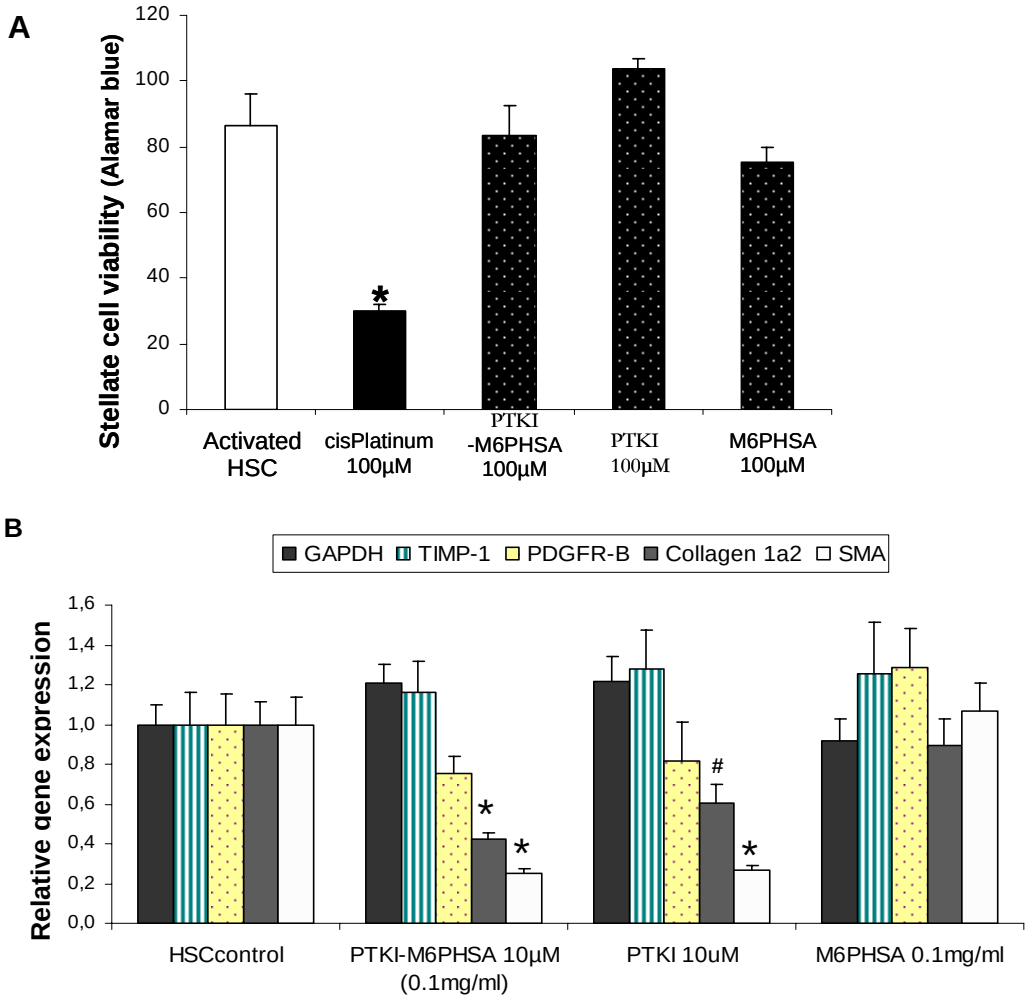

Figure 2. Activated HSC incubated with PTKI-M6PHSA.

*A. Effect of PTKI-M6PHSA and PTKI on HSC cell viability, as determined by Alamar Blue viability assay. Indicated concentrations reflect the platinum content of the conjugate, or equivalent amounts cisplatin, PTKI or M6PHSA. Cultured HSC were incubated for 24h with the compounds (*P<0.01).*

*B. Activated HSC gene expression after incubation with PTKI-M6PHSA, PTKI and M6PHSA. Concentrations denote the amount of PTKI (10 µM) or the corresponding amount of M6PHSA carrier (0.1mg/ml). Gene expressions levels were normalized to the expression of GAPDH and subsequently normalized to the relative expression of control cells (*P<0.01 and #P<0.05).*

Cells

Hepatic stellate cells were isolated from male Wistar rat livers by the pronase-collagenase method followed by a density centrifugation on a 12% Nycodenz gradient according to Geerts et al (20;21)(Hepatol 1998). The isolated stellate cell fraction was cultured in 6 well-plates (Corning) in Dulbecco's Modified Eagle's Medium (Gibco, Life technologies Ltd.) supplemented with 10% fetal calf serum, 100 U/ml penicillin and 100 mg/ml streptomycin in a 5% CO_2 humidified atmosphere at 37°C. Cells were split after 3 days and cultured until day 10 to obtain the activated HSC phenotype, and these culture activated HSC were used for the experiments described below.

Cell viability studies

Activated HSC (10,000 cells/well seeded in 96 well-plates, Corning) were washed with serum-free medium and incubated for 24h in medium supplemented with 100 μM PTKI, PTKI-M6PHSA (1mg/ml, corresponding to 100 μM of PTKI) or M6PHSA (1mg/ml). During the last 2h of the incubations, Alamar blue reagent (Serotec, Oxford, UK) was added in a proportion of 10% of the volume per well. Viability of the cells was determined fluorimetrically according to the supplier's instructions.

Effects on gene expression

The potential antifibrotic activity of PTKI-M6PHSA and PTKI was evaluated in cultured HSC and in precision-cut liver slices of fibrotic rat livers.

Activated HSC were incubated as described above with PTKI (10 μM), PTKI-M6PHSA (0.1mg/ml, corresponding to 10 μM of PTKI), or M6PHSA (0.1 mg/ml) for 24h, after which they were processed for RNA analysis as described below. A total of four independent experiments were performed in HSC cultures from four different Wistar Male rats.

Precision-cut liver slices were prepared as described elsewhere (22;23). Briefly, precision-cut liver slices (8mm diameter, 250μm) from fibrotic livers of BDL3 rats (week 3 after BDL) were prepared using a Krumdieck tissue slicer and stored in University of Winconsin preservation solution (UW) on ice until further use.

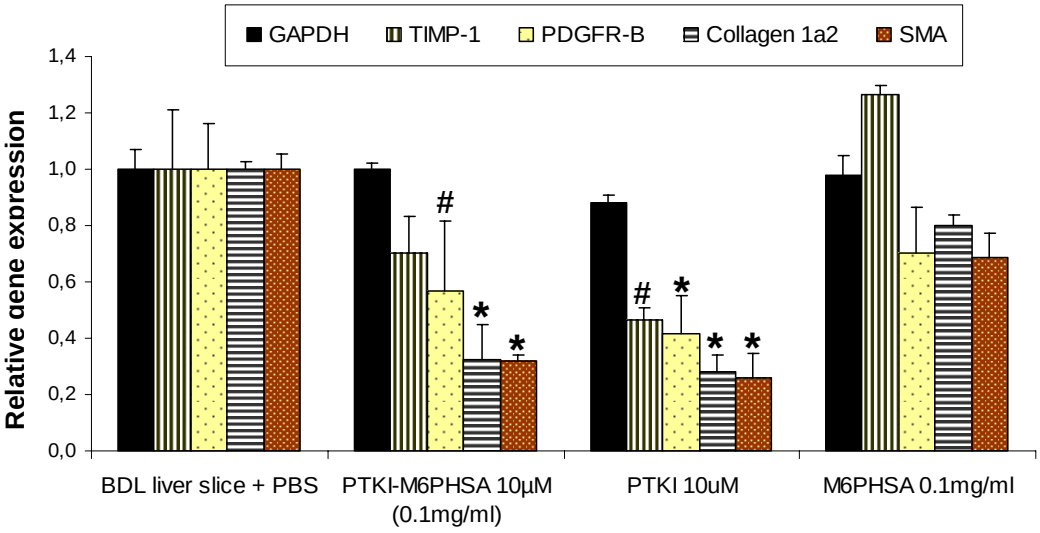

Figure 3. Effect on gene expression of PTKI-M6PHSA on BDL3 liver slices. *Concentrations denote the amount of PTKI (10 µM) or the corresponding amount of M6PHSA carrier (0.1mg/ml). Gene expression levels of control slices were normalized versus GAPDH and subsequently normalized versus the expression levels in control fibrotic liver slices (*$P<0.01$ and $^{\#}P<0.05$).*

Slices were preincubated for 2 h in William's medium E (Gibco, Life technologies Ltd., Paisley, Scotland, UK) supplemented with D-glucose (25mM) and gentamycin (50 mg/ml) and saturated with 95% O_2, 5% CO_2 at 37°C. Slices were transferred into fresh medium and incubated individually in six-well plates with PTKI-M6PHSA (0.1 mg/ml, corresponding to 10 µM of PTKI), PTKI (10 µM) or M6PHSA (0.1 mg/ml). After 24 h of incubation, slices were snap-frozen in liquid nitogen (real-time PCR analysis). Each measurement was performed on three liver slices from the same liver and the experiment was repeated on livers from three different BDL3 rats.

Animal experiments

All animal studies were approved by the local committee for care and use of laboratory animals at Groningen University, and were performed according to strict governmental and international guidelines on animal experimentation. Animals had free access to tap water and standard lab chow and were housed in a 12h/12h light/dark cycle. All the animals included in these studies were monitored by analysis of body weight (BW) and biochemical parameters reflecting liver functions like serum bilirubin levels, AST, ALT, AP and gamma-GT levels. These analyses were performed at the University Medical Center Groningen by standard biochemical procedures.

BDL model

Liver fibrosis was induced in male Wistar rats (250 g, Harlan, Zeist, The Netherlands) by bile duct ligation as described previously (24). Briefly, rats were anesthesized with isoflurane (2% isoflurane in 2:1 O_2/N_2O, 1 L/min) (Abbot Laboratories Ltd., Queensborough, UK). After midline laparotomy, the common bile duct was ligated by double ligature with 4-0 silk and transected between the two ligations. Animals were allowed to recover and carefully observed until final sacrifice at the end of the experiments.

Distribution study

At day 10 after BDL, rats received a single intravenous injection of PTKI-M6PHSA (3.3 mg/kg, corresponding to 150 μg PTKI/kg). Control animals were injected with an equivalent volume of the vehicle (saline, 250 μl). Animals were sacrificed 2h post injection of the compounds. Organs were harvested and processed for immunohistochemical detection of the conjugate as described below.

Single dose effect study

At day 10 after BDL, rats received a single intravenous injection of 3.3 mg/kg PTKI-M6PHSA or saline. Animals were sacrificed day 11 or 12 post injection of the compounds. Blood and organs were harvested and processed for analysis of serum markers, RNA isolation and immunohistochemical analysis as described below.

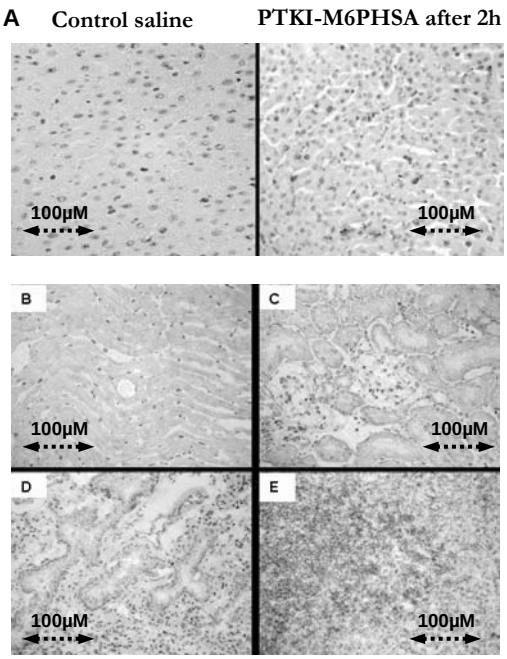

Figure 4. Localization of PTKI-M6PHSA in different organs and liver. *Immunostaining with Anti-HSA of different organs from rats treated with PTKI-M6PHSA after 2hours of PTKI-M6PHSA single administration. A. liver; B. heart; C. kidney; D. lung; E. spleen. Immunostaining with Anti-HSA of liver tissue from rats treated with PTKI-M6PHSA at different time points after single administration: control saline; 2h; 24h; 48h. Magnification, 20x.*

Multiple dose study

Starting at day 10 after BDL, rats received four daily intravenous injections of PTKI-M6PHSA (3.3 mg/kg, corresponding to 150 µg PTKI/kg), free PTKI (150 µg/kg) or saline. PTKI was dissolved first in DMSO at a concentration of 15 mg/ml and subsequently diluted to a concentration of 0.25 mg/ml with Hydroxy propyl-B-cyclodextrin (ENCAPSIN, Janssen Biotech 30-222-55) 20% w/v (pH adjusted to 3.0 with 1M HCl). The final dosage of DMSO was less than 0.05%. Animals were treated again every 24h, and received a total of 4 doses until they were sacrificed at day14 after BDL (24h post injection of the last dose). A control group of animals was sacrificed at day 10,

i.e. just before start of the treatments. Blood and organs were harvested and processed similar as for single dose effect studies.

	BDL day 10 control saline	**BDL day 14 control saline**	**BDL day 14 + PTKI-M6PHSA**	**BDL day 14 + PTKI**
Number of rats	5	6	5	6
Body weight (g)	250.2 ± 46.7	290.4 ± 9.6	273.4 ± 16.4	280.7 ± 10.1
Liver/body ratio (g/g)	0.055 ± 0.009	0.060 ± 0.009	0.063 ± 0.011	0.060 ± 0.004
Dose	saline	saline	150 ug/kg (PTKI conc) or 3.3mg/kg (prot conc)	150 ug/kg
Bilirubin (umol/l)	183.7 ± 35.8	152.0 ± 14.2	187.4 ± 35.7	156.5 ± 32.8
ALT (U/l)	86.3 ±30.9	118.5 ±46.9	117.6 ±32.3	121.3 ±34.2
Alkaline Phosp (U/l)	391.2 ±46.4	405.2 ±46.0	478.6 ±132.9	410.0 ±91.2

Table 2. Dose regimens, animal data and biochemical serum parameters from PTKI-M6PHSA multiple administration study. *Data are shown as mean ± SD. BDL, bile duct animals.*

RNA isolation and gene expression analysis

Total RNA was isolated from cells or liver slices using an RNA isolation kit (Qiagen GmbH, Hilden,Germany) according to the manufacturer's procedures. Isolation of RNA from liver tissue was performed using Trizol (manufacturer). The amount of RNA was estimated with a Nanodrop system (ND-1000 Spectrophotometer, NanoDrop Technologies, Wilmington, DE). cDNA was synthesized from similar amounts of RNA

using Superscript III first strand synthesis kit (Invitrogen life technology, Carlsbad, CA). The reverse transcriptase reaction was performed for 5min at 65°C, 10 min at 25°C, 50 min at 50°C and 5 min at 85°C with random primers. Quantitative Real-time RT-PCR was performed in duplicate on a ABI 7900HT system (Applied Biosystems, Foster City, CA) using SYBR green primers. 1μl of cDNA solution corresponding to approximately 0.5μg was added in each PCR reaction as well as 10μl of SYBR Green PCR Master Mix (Applied Biosystems) and the forward and reverse primers (50 μM). For each sample, 1 μl of cDNA was mixed with 0.4 μl of each gene-specific primer (50 μM), 0.8 μl DMSO, 8.4 μl water and 10 μl SYBR Green PCR Master Mix. The housekeeping gene Glyceraldehyde-3-phosphate dehydrogenase (GAPDH) was used as a reference gene and for normalization of the other genes, while ultrapure water was used as a negative control.

The following primers were used to investigate antifibrotic responses: rat smooth muscle α actin forward, 5'-GACACCAGGGAGTGATGGTT -3', reverse, 5'-GTTAGCAAGGTCGGATGCTC-3' (product size 202 bp); rat collagen type 1 a1 (collagen 1 a1) forward, 5'-AGCCTGAGCCAGCAGATTGA-3', reverse, 5'-CCAGGTTGCAGCCTTGGTTA-3', (product size 145 bp); rat PDGFR-β forward, 5'-TGTTCGTGCTATTGCTCCTG -3', reverse, 5'-TCAGCACACTGGAGAAGGTG -3', (product size 201 bp); rat timp-1 forward, 5'-GAGAGCCTCTGTGGATATGT -3', reverse, 5'-CAGCCAGCACTATAGGTCTT -3', (product size 334 bp); and rat GAPDH forward 5'-CGCTGGTGCTGAGTATGTCG-3', reverse, 50-CTGTG GTCATGAGCCCTTCC-30, (product size 179 bp). PCR reactions consisted of 40 cycles (denaturation 15 s 95°C, annealing 15 s 56°C, extension 40 s 72°C). The formation of single products was confirmed by analyzing the dissociation step at the end of each PCR reaction.

Analysis of hepatic gene expression

RNA was isolated from frozen liver samples using an RNA isolation kit (Qiagen GmbH, Hilden,Germany). Quantitative PCR was performed as described above with primers for rat collagen α1 (II), smooth muscle α-actin, PDGFR-β, tissue inhibitor metalloproteinase type 1 (TIMP-1) and GAPDH (Applied Biosystems, Foster City, CA). Real-time PCR was

carried out on an ABI PRISM 7900HT. Data were analyzed with the SDS 2.1 software program (Applied Biosystems). The relative amount of the designated PCR product was calculated by the comparative threshold cycle (CT) method and referred to control treatment.

Immunohistochemical analyses

Cryostat sections (4 μm) of liver, heart, kidney, lung and spleen were acetone-fixed and stained for the presence of the PTKI-M6PHSA conjugate with an antibody directed against HSA (Cappel ICN Biomedicals, Zoetermeer, The Netherlands) as described elsewhere (24).

The degree of hepatic fibrosis was estimated as the percentage of area of each section (4μm) stained positive with picro Sirius Red in saturated picric acid (both from Sigma). The amount of fibrogenic myofibroblasts was estimated by measuring the percentage of area stained with anti-smooth muscle α actin (αSMA, Sigma, Gillingham, UK) in 10 randomly selected high power fields per sample. An optic microscope (Olympus BX40) connected to a high-resolution camera (Olympus Camedia C-5050 zoom) was used for morphometric assessment of percentage of area with positive staining. Microphotographs were taken at an original magnification of 4x10. The fibrotic area per liver section was quantified by morphometric analysis of the sections using the Image J software package (NIH, Bethesda, ML, USA) and images were captured following automatic white balance and light intensity equilibration with a 40 × magnification objective and digitized as RGB 24-bit. After shading correction and interactive thresholding, the selected positive pixels were measured. The positive area was the sum of the area of positive pixels per liver biopsy. Results were calculated as the average area of positive pixels per liver biopsy and divided into each group of animal treatment.

Statistical analysis

Results are expressed as the mean of at least three independent experiments ± SD, unless otherwise indicated. Statistical analysis was performed with an unpaired Student's t-test and differences were considered significant at $p<0.05$.

Results

Synthesis and characterization of PTKI-M6PHSA conjugate

When observing the structure of PTKI (Figure 1A) or the related kinase inhibitor imitanib, it is clear that the structure is mainly composed of aromatic rings lacking functional groups that can be used for drug linking purposes. In general, drug conjugation protocols often start with the preparation of a drug-linker adduct at carboxyl, hydroxyl, thiol or primary amino groups. Since this is not possible for PTKI, we applied a novel type of platinum-based drug linker that conjugates the drug via a coordinative linkage at one of the pyridyl nitrogens (Figure 1A). HPLC analysis and mass spectrometry indicated complete derivatization of the drug into the drug-ULS 1:1 product. The PTKI-ULS adduct was subsequently conjugated to M6PHSA and the final high-molecular weight product was extensively purified by dialysis, which also removed free PTKI-ULS molecules not linked to the carrier (HPLC analysis, data not shown). Summarizing the two reaction steps, an overall yield of 84% was reached for the synthesis of PTKI-M6PHSA (Figure 1A). An average of eight PTKI-ULS molecules was coupled per M6PHSA, as determined by HPLC after release of the drug from the carrier. Conjugation of PTKI to M6PHSA did not change the charge or size features of M6PHSA, as assessed by anion-exchange chromatography and size exclusion chromatography, respectively (Figure 1B).

Effect of PTKI-M6PHSA on cultured stellate cells

The use of ciplatinum as a linker may introduce platinum-associated effects in the drug targeting preparation. We therefore evaluated PTKI-ULS-M6PHSA for its effect on HSC viability. In contrast to free cisplatin, which clearly displayed toxic effects, PTKI-M6PHSA, PTKI and M6PHSA did not reduce the viability of HSC after 24h treatment (Figure 2A).

To examine the potential antifibrotic effects of PTKI-M6PHSA conjugate and non-conjugated PTKI on activated HSC, we investigated the expression of fibrosis related genes in cultured HSC by quantitative RT-PCR. PTKI-M6PHSA downregulated the

expression of α-SMA and collagen α1 (II) by 80% and 60% respectively, and PTKI reduced the expression of the same genes with a similar potency (figure 2B). In contrast, M6PHSA did not affect the expression of these genes in HSC. The other genes that were examined, PDGFR-β or TIMP-1, were not significantly reduced by either treatment.

Effect of PTKI-M6PHSA on BDL3 liver slices

In addition to cultured cells, we also used another *in vitro* system, which encompasses all liver cell types (hepatocytes, HSC, Kupffer cells and liver endothelial cells) in the context of their natural environment and extracellular matrix (22). We incubated precision-cut slices from fibrotic BDL rat livers (BDL3 slices) with PTKI-M6PHSA, PTKI or M6PHSA and measured the impact of the compounds on gene expression by real-time PCR.

Interestingly, PTKI-M6PHSA and PTKI had similar effects in liver-slices treatment and cultured HSC (Figure 3). A significant suppression of collagen α1 (II), α-smooth muscle actin, PDGFR-β and TIMP-1 mRNA levels by PTKI (80%; 70%; 60%, $p<0.01$ and 50%, $p<0.05$, respectively) and PTKI-M6PHSA (70%; 70%, $p<0.01$; 40%, $p<0.05$, respectively) was found after evaluation of mRNA expression levels.

Animal studies

Table 1 shows the animal characteristics after a single injection study of PTKI-M6PHSA or vehicle. Administration of PTKI-M6PHSA did not affect the body weight of the treated BDL rats versus non-treated. None of the biochemical parameters analyzed were significantly changed.

Distribution of PTKI-M6PHSA in fibrotic rats

Previous studies in our laboratory have demonstrated that M6PHSA binds to and is taken up by activated HSC in the fibrotic liver. Typically, about 60% of the injected dose accumulated in the fibrotic liver already within 10 min after administration, in a non-parenchymal distribution pattern (17). The present study confirms this accumulation of PTKI-M6PHSA in the liver 2h after administration (Figure 4A), while the construct was undetectable in other organs like heart, kidney, lung and spleen. (Figure 4B-E). As shown

in Figure 4A (right panel), the staining in the liver reflects non-parenchymal cell distribution, with hardly any accumulation of the product in the hepatocytes. These results suggest that the coupling of PTKI-ULS did not alter the distribution of the HSC-selective carrier *in vivo*.

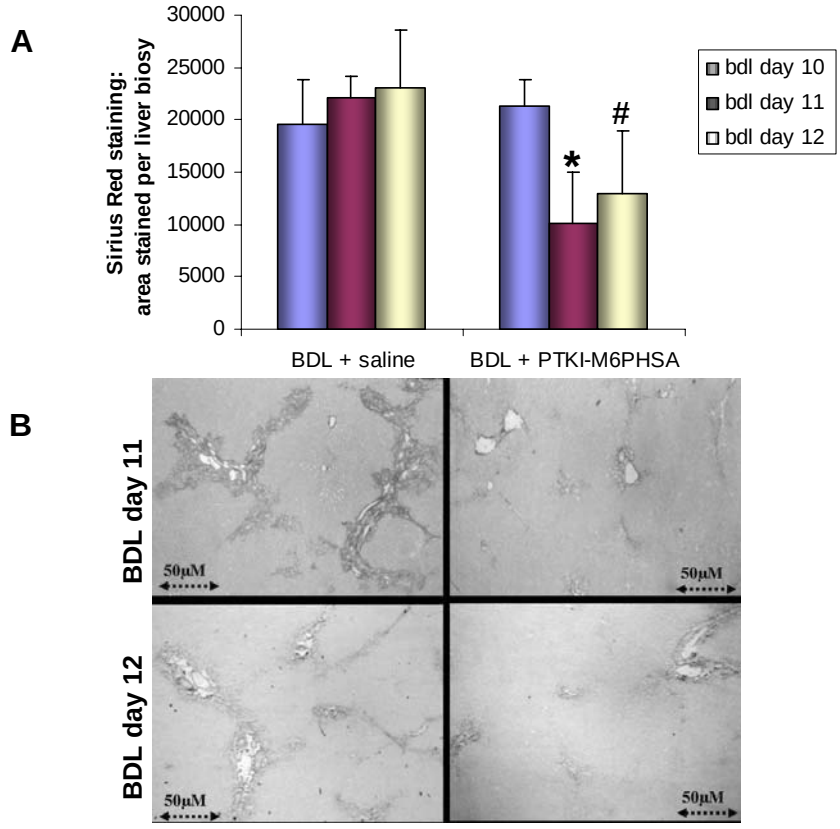

Figure 5. Effect of PTKI-M6PHSA single administration to BDL rats on the deposition of collagen in the liver, as assessed by Sirius Red staining.

*A. Quantification of the area with Sirius Red staining in rat liver specimens (n = 25, mean±sd ttest between saline and drug treated groups:*P<0.01 and #P<0.05 vs. BDL saline control). B. Liver sections were processed for immunohistochemistry and then stained with Sirius Red. Rats receiving saline (left column) showed a marked deposition of collagen, as assessed with Sirius Red, which co-localized with areas with active fibrogenesis. However, rats treated with PTKI-M6PHSA (right column) showed*

attenuated liver fibrosis development. Magnification (40x) photomicrograph of liver sections from bile duct ligated rats on day 10 and 11 post BDL (i.e. 24h and 48h after administration, respectively).

Effects of PTKI-M6PHSA in fibrotic rats

Antifibrotic effects of PTKI-M6PHSA were studied in two different experimental set-ups. First, we investigated whether a single dose of the product would affect fibrotic gene expression, in a similar approach as described above for cultured HSC and precision-cut slices. We did not observe changes in the expression of the chosen reporter genes for fibrosis (data not shown). Immunohistochemical staining of fibrotic markers, however, clearly indicated pharmacological activity of the delivered drug. Sirius Red staining for collagen showed a continuous increment in deposited extracellular matrix components between day 10 to 12 after bile duct ligation (Figure 5A). Treatment with a single dose of PTKI-M6PHSA significantly attenuated collagen deposition both 24h and 48h after administration ($p<0.01$; $0<0.05$, respectively) (Figure 5B). Apart from reduced staining intensity, the antifibrotic effect of PTKI-M6PHSA was also illustrated by a reduced portal-portal bridging in fibrotic areas.

Smooth muscle α-actin staining (αSMA) showed an increased number of αSMA-positive cells between days 10 and 12, which correlates with the exacerbation of liver fibrosis upon prolonged BDL (Figure 6A). Treatment of BDL rats with PTKI-M6PHSA significantly attenuated the number of activated HSC stained areas at 24h and 48h respectively (Figure 6B, $p<0.01$).

After completion of the single dose study, we continued our pharmacological evaluation with a multiple dose study in the same model. Apart from testing of the conjugate PTKI-M6PHSA, we now also included the free drug at a dose equivalent to the amount of PTKI in the conjugate (150 μg/kg). Such a low dosage will not necessarily be therapeutically effective, in view of the necessary dose of 5 to 20 mg/kg of imitanib in other studies (12;25). Animal characteristics of the multiple dose study are included in Table 2.

We analyzed mRNA expression levels for collagen-α1 (II), smooth muscle α-actin, PDGFR-β and TIMP-1 and found no significant differences between treated and

untreated animals of study. Also collagen deposition and α- SMA expression was not different between those groups (Table 3).

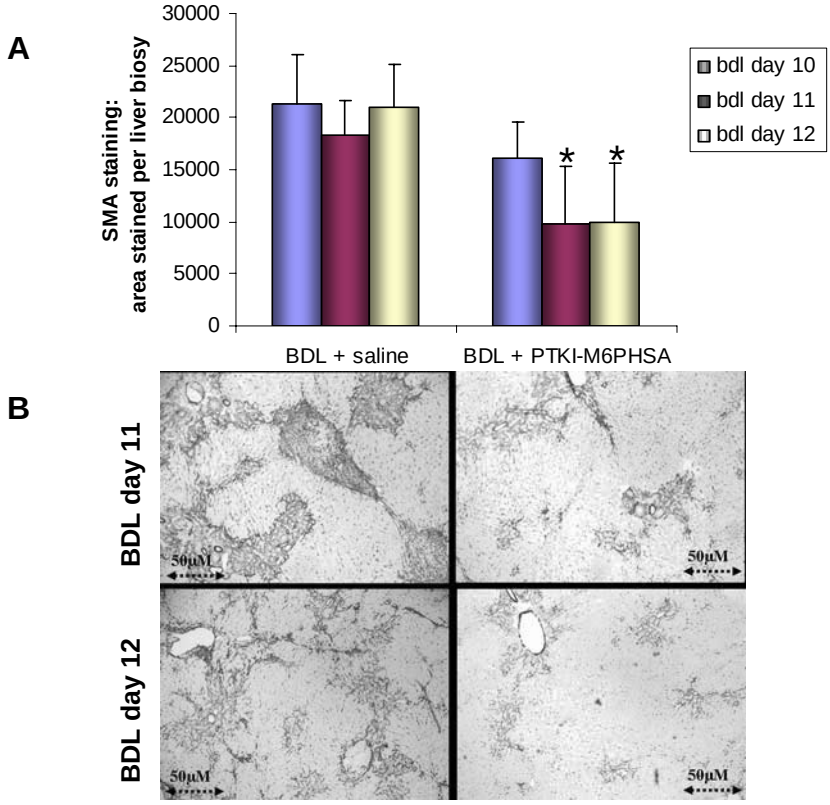

Figure 6. Effect of PTKI-M6PHSA single administration to BDL rats on the accumulation of myofibroblasts and activated HSC, as assessed by smooth muscle α-actin expression (αSMA).

*A. Quantification of the area with αSMA staining in rat liver specimens (n = 25, mean±sd ttest between saline and drug treated groups:*P<0.01 vs. BDL saline control).*

B. Liver sections were processed for immunohistochemistry and then stained with anti-αSMA antibody. Rats receiving saline (left panels) showed a marked accumulation of αSMA-positive cells, which co-localized with areas with active fibrogenesis. However, rats treated with PTKI-M6PHSA (right panels) showed less quantity of αSMA-positive cells. Magnification (40x) photomicrograph of liver sections from bile duct ligated rats on day 10 and 11 post BDL (i.e. 24h and 48h after administration, respectively)

Discussion

Liver fibrosis is in principle a reversible process in which the stellate cells have been identified as the key fibrogenic cells (26). PDGF is the most potent mitogen for HSC *in vitro*, and it plays an important role in the transformation of HSC into myofibroblast-like cells *in vivo* (27). Targeting the PDGF signalling cascade therefore represents a promising antifibrotic approach. In the present study, we employed a kinase inhibitor with a closely related structure to imatinib (Gleevec, Novartis). The antifibrogenic properties of the latter well-known kinase inhibitor have already been described (10;12). On the other hand, concerns have been raised in relation to the effectiveness of imatinib as an antifibrogenic drug (13), especially in later stages of fibrosis. The new product PTKI-M6PHSA was designed to effectively and specifically deliver the inhibitor to HSC, in order to improve its antifibrotic properties. In the present study, we demonstrate the antifibrogenic effects of PTKI-M6PHSA in two different and validated *in vitro* systems and in the BDL model of liver fibrosis.

We confirmed that PTKI showed a similar antifibrotic potential as imatinib by incubating the drug with culture-activated HSC and precision-cut liver slices. In both test systems, PTKI potently inhibited the gene expression of fibrotic markers. The observed effect is presumably attributed to the blockade of PDGF's profibrogenic and mitogenic actions since the growth factor is synthesized *in situ* by the activated HSC in culture or in slices (28). Furthermore, PTKI is a very potent inhibitor of PDGFR-kinase with an IC50 of 10 nM (15). We also found that PTKI reduced PDGFR-β and TIMP-1 expression. TIMP-1 expression is increased during liver fibrosis and plays an important role in liver fibrogenesis by modulating extracellular matrix remodelling (29). More importantly, PTKI-M6PHSA had similar pharmacological effects as PTKI in activated HSC and fibrotic liver slices. These results suggest that the drug is effectively released from the carrier during the incubation period, and is capable of inhibiting the PDGF-R kinase pathway.

Having established the antifibrotic potential of the conjugate, we confirmed *in vivo* homing of PTKI-M6PHSA from the circulation to the fibrotic liver. Similar to findings with other drug-M6PHSA conjugates (19;30) we detected its presence in non-parenchymal cells by anti-HSA immunostaining. These findings suggest that PTKI-M6PHSA is mainly delivered within the fibrotic organ in BDL rats and therefore is associated with HSC. Assuming that PTKI-M6PHSA behaves similar to other drug targeting preparations that encompass the ULS linker, we can expect a slow release of PTKI during days rather than hours, providing continuous local drug levels (19) (Prakash, SB-LZM paper2006, Temming RGD-PEG-SB-HSA paper2006).

Several approaches for a blockade of the PDGF signaling have been investigated as a strategy to block the ongoing liver fibrotic process. Some papers showed that monoclonal antibodies directed against the extracellular domain of the PDGF receptor can prevent binding of the PDGF ligand, thereby inhibiting mitogenic signaling (31;32). Consistent with this, Kinnman and colleagues (9) described that imatinib inhibited PDGF-BB induced proliferation of HSC *in vitro*, but a short-term treatment *in vivo* did not completely blunt HSC proliferation 48 hours after BDL. In a different strategy, Borkham-Kamphorst and colleagues produced a soluble antifibrogenic protein drug, sPDGFRB, and observed a reduction in ECM deposition after daily administration fourteen days after BDL (33). According to Neef and colleagues (13) this effect of imatinib is limited to the early phase of fibrogenesis, due to the lack of efficiency in advanced liver injury, i.e., 3 to 4 weeks after BDL. In contrast to this latter observtions, there is another study where a pronounced inhibition of SMA-positive cells is found after 8 weeks of imatinib administration (12). These authors found a marked attenuation of the liver fibrosis in the pig-serum induced model of liver fibrosis, characterized by a slow progression of fibrogenesis, resembling the human situation. Thus, it might be a relevant therapy in patients with early stages of liver fibrosis.

Our strategy differs completely from the above listed studies in which the free drug imatinib is used (10;12). We employed a carrier, M6PHSA that is internalized by the target HSC and releases the kinase inhibitor inside the cells.

After single administration, PTKI-M6PHSA markedly reduced collagen deposition together with a suppression of αSMA-positive cells number which reflects activated HSC (34). In contrast to the effects on protein levels, PTKI-M6PHSA administered to BDL animals did not affect the gene expression of the fibrotic markers. This discrepancy either reflects different sensitivity of the assays, or corresponds to a greater reduction of collagen and αSMA at the protein level than at gene expression level. This divergence has previously been described in experiments investigating the inhibition of hepatic fibrosis (35), and might be due to post-transcriptional regulation of collagen expression in cultured HSC (36).

The observation that antifibrotic effects are discernable even 48h after a single dose suggests that effective PTKI levels are present during a prolonged period of time. In previous studies with other ULS-based conjugates, we have observed a slow drug release pattern from the ULS linker that may afford continuous drug release during a period of days (19). The proposed mechanism is competitive displacement of the drug by S-donor ligands like glutathione and ligands containing sulfur atoms (e.g. methionine) or aromatic nitrogens (nucleotides, histidine). After binding of PTKI-M6PHSA to HSC and its internalization, the release of PTKI from the conjugate is a critical point for exerting the inhibitory effect on PDGF-R kinase. The release of PTKI may occur in the lysosomes, the compartment to which M6PHSA is routed after internalization (37). Hence, a continued release of PTKI from the conjugate would be available and a sustained blockade of PDGF kinase activity may be achieved. In the present study, PTKI-M6PHSA produced a significant effect on the fibrotic process 24 to 48 hours after its administration to BDL rats. These results are in good agreement with the previously hypothesized release kinetics of our drug-conjugates. Furthermore, it suggests the possibility of employing PTKI-M6PHSA as a depot from which the drug is released for a prolonged period of time.

Our data are in good agreement with the studies of Neef and colleagues. Yet, after multiple dose administration of PTKI-M6PHSA, the collagen and αSMA protein expression was not decreased while the results mentioned above show that the process of liver fibrosis development is clearly decreased by a single dose of PTKI-M6PHSA. How

can this unexpected lack of effect after repeated administration of our drug-targeting conjugate be explained? We propose that this may be due to the activation of alternative cytokine pathways that compensates for the inhibition of PDGF-R cascade (38).

	Parameter analyzed	BDL day 10 + control saline	BDL day 14 + control saline	BDL day 14 + PTKI-M6PHSA	BDL day 14 + PTKI
Gene expression (fold induction)	GAPDH	1.1 ± 0.4	1.3 ± 0.6	0.8 ± 0.2	1.3 ± 0.4
	α-SMA	0.8 ± 0.4	1.1 ± 0.7	1.2 ± 0.3	1.1 ± 0.3
	Collagen	0.8 ± 0.3	1.3 ± 0.3	1.2 ± 0.4	1.2 ± 0.5
	PDGF Receptor	1.0 ± 0.3	3.2 ± 2.4	3.2 ± 1.9	2.6± 0.6
Protein expression (staining intensity)	Sirius Red staining	++	+++	+++	+++
	αSMA staining	++	+++	+++	+++

Table 3. Effect of PTKI-M6PHSA multiple administration to BDL rats. *Data are shown as mean ± SD.*

Redundancy of regulatory pathways is a common feature in the fibrotic process. Especially if the causative agent of liver fibrosis is not removed, the specific inhibition of PDGF-R on the hepatic stellate cells may temporarily affect the proliferation of HSC and collagen deposition, as we observed after single injection of PTKI-M6PHSA, but not after prolonged administration of PDGF-R inhibitor. Long-term administration of PTKI-M6PHSA may allow enough time for the activation of alternative pathways, such as TGF-

β, that may compensate for the inhibition of PDGF cascade (13). Albeit other compensatory mechanisms are also possible, this would also suggest that the combined elimination of more than one pathway could lead to an effective inhibition of hepatic fibrosis (33). For example, simultaneous inhibition of PDGF and TGF-β cascade might be more appropriate strategy to attenuate the process of liver fibrosis. Recent experiments explaining this approach showed that it was more effective than inhibition of either pathway alone (39). A TGF-β receptor kinase inhibitor has been described and cell-selective delivery of this construct to the kidney is now being examined in our laboratory (Prakash, manuscript in preparation). Consequently, targeting both cascades would be an eligible approach in future investigations.

In conclusion, the data presented in the present study provide evidence that PTKI-M6PHSA is effective *in vitro* and specifically taken up by non-parenchymal cells in the liver, during fibrosis. Single dose administration of PTKI-M6PHSA proved to be an effective antifibrotic strategy *in vivo*, although prolonged administration did not reveal significant effects. Cell-selective elimination of multiple signalling pathways may provide a tool to design novel strategies.

Acknowledgements

This study was supported by grants from SenterNovem (TSGE1083), NWO Science Netherlands (R 02-1719, 98-162). Jan Visser and Jai Prakash (University of Groningen, The Netherlands) are kindly acknowledged for assistance in HPLC analysis and colleagues at Kreatech for critical reading of the manuscript.

Reference List

1. Tsukada,S., Parsons,C.J., and Rippe,R.A. 2006. Mechanisms of liver fibrosis. *Clin. Chim. Acta* **364**:33-60.

2. Friedman,S.L. 1999. The virtuosity of hepatic stellate cells. *Gastroenterology* **117**:1244-1246.

3. Pinzani,M. 2002. PDGF and signal transduction in hepatic stellate cells. *Front Biosci.* **7**:d1720-d1726.

4. Wong,L., Yamasaki,G., Johnson,R.J., and Friedman,S.L. 1994. Induction of b-platelet-derived growth factor receptor in rat hepatic lipocytes during cellular activation in vivo and in culture. *J. Clin. Invest.*1563-1569.

5. De Bleser,P.J., Jannes,P., Van Buul-Offers,S.C., Hoogerbrugge,C.M., Van Schravendijk,C.F.H., Niki,T., Rogiers,V., Van den Brande,J.L., Wisse,E., and Geerts,A. 1995. Insulinlike growth factor-II/mannose 6-phosphate receptor is expressed on CCl4-exposed rat fat-storing cells and facilitates activation of latent transforming growth factor-b in cocultures with sinusoidal endothelial cells. *Hepatol* **21**:1429-1437.

6. Weiner,J.A., Chen,A., and Davis,B.H. 2000. Platelet-derived growth factor is a principal inductive factormodulating mannose 6-phosphate/insulin-like growth factor-II receptorgene expression via a distal E-box in activated hepatic stellate cells. *Biochem. J.* **345 Pt 2**:225-231.

7. Bachem,M.G., Meyer,D., Schäfer,W., Riess,U., Melchior,R., Sell,K.M., and Gressner,A.M. 1993. The response of rat liver perisinusoidal lipocytes to polypeptide growth regulator changes with their transdifferentiation into myofibroblast-like cells in culture. *J. Hepatol.* **18**:40-52.

8. von,M.M. 2005. Targeted therapy with imatinib: hits and misses? *J. Clin. Oncol.* **23**:8-10.

9. Kinnman,N., Goria,O., Wendum,D., Gendron,M.C., Rey,C., Poupon,R., and Housset,C. 2001. Hepatic stellate cell proliferation is an early platelet-derived growth factor-mediated cellular event in rat cholestatic liver injury. *Lab Invest* **81**:1709-1716.

10. Buchdunger,E., Cioffi,C.L., Law,N., Stover,D., Ohno-Jones,S., Druker,B.J., and Lydon,N.B. 2000. Abl protein-tyrosine kinase inhibitor STI571 inhibits in vitro signal transduction mediated by c-kit and platelet-derived growth factor receptors. *J. Pharmacol. Exp. Ther.* **295**:139-145.

11. Buchdunger,E., Zimmermann,J., Mett,H., Meyer,T., Muller,M., Regenass,U., and Lydon,N.B. 1995. Selective inhibition of the platelet-derived growth factor signal transduction pathway by a protein-tyrosine kinase inhibitor of the 2-phenylaminopyrimidine class. *Proc. Natl. Acad. Sci. U. S. A* **92**:2558-2562.

12. Yoshiji,H., Noguchi,R., Kuriyama,S., Ikenaka,Y., Yoshii,J., Yanase,K., Namisaki,T., Kitade,M., Masaki,T., and Fukui,H. 2005. Imatinib mesylate (STI-571) attenuates liver fibrosis development in rats. *Am. J. Physiol Gastrointest. Liver Physiol* **288**:G907-G913.

13. Neef,M., Ledermann,M., Saegesser,H., Schneider,V., Widmer,N., Decosterd,L.A., Rochat,B., and Reichen,J. 2006. Oral imatinib treatment reduces early fibrogenesis but does not prevent progression in the long term. *J. Hepatol.* **44**:167-175.

14. Bataller,R., and Brenner,D.A. 2005. Liver fibrosis. *J. Clin. Invest* **115**:209-218.

15. Zimmermann,J., Buchdunger,E., Mett,H., Meyer,T., and Lydon,N.B. 1997. Potent and selective inhibitors of the abl-kinase:phenylamino-pyrimidine (PAP) derivatives. *Bioorganic & Medicinal Chemistry Letters* **7**:187-192.

16. Beljaars,L., Meijer,D.K., and Poelstra,K. 2002. Targeting hepatic stellate cells for cell-specific treatment of liver fibrosis. *Front Biosci.* **7**:e214-e222.

17. Beljaars,L., Molema,G., Weert,B., Bonnema,H., Olinga,P., Groothuis,G.M.M., Meijer,D.K.F., and Poelstra,K. 1999. Albumin modified with mannose 6-phosphate: A potential carrier for selective delivery of antifibrotic drugs to rat and human hepatic stellate cells. *Hepatol* **29**:1486-1493.

18. van Gijlswijk,R.P., Talman,E.G., Janssen,P.J., Snoeijers,S.S., Killian,J., Tanke,H.J., and Heetebrij,R.J. 2001. Universal Linkage System: versatile nucleic acid labeling technique. *Expert. Rev. Mol. Diagn.* **1**:81-91.

19. Gonzalo,T., Talman,E.G., van,d., V, Temming,K., Greupink,R., Beljaars,L., Reker-Smit,C., Meijer,D.K., Molema,G., Poelstra,K. et al 2006. Selective targeting of pentoxifylline to hepatic stellate cells using a novel platinum-based linker technology. *J. Control Release* **111**:193-203.

20. Beljaars,L., Weert,B., Geerts,A., Meijer,D.K.F., and Poelstra,K. 2003. The preferential homing of a platelet derived growth factor receptor-recognizing macromolecule to fibroblast-like cells in fibrotic tissue. *Biochem. Pharmacol.* **66**:1307-1317.

21. Geerts,A., Niki,T., Hellemans,K., De Craemer,D., Van den Berg,K., Lazou,J.-M., Stange,G., Van de Winkel,M., and De Bleser,P.J.

1998. Purification of rat hepatic stellate cells by side scatter-activated cell sorting. *Hepatol* **27**:590-598.

22. Olinga,P., Merema,M.T., de Jager,M.H., Derks,F., Melgert,B.N., Moshage,H., Slooff,M.J., Meijer,D.K., Poelstra,K., and Groothuis,G.M. 2001. Rat liver slices as a tool to study LPS-induced inflammatory response in the liver. *J. Hepatol.* **35**:187-194.

23. van de,B.M., Groothuis,G.M., Draaisma,A.L., Merema,M.T., Bezuijen,J.I., van Gils,M.J., Meijer,D.K., Friedman,S.L., and Olinga,P. 2005. Precision-cut liver slices as a new model to study toxicity-induced hepatic stellate cell activation in a physiologic milieu. *Toxicol. Sci.* **85**:632-638.

24. Beljaars,L., Poelstra,K., Molema,G., and Meijer,D.K.F. 1998. Targeting of sugar- and charge-modified albumins to fibrotic rat livers: the accessibility of hepatic cells after chronic bile duct ligation. *J. Hepatol.* **29**:579-588.

25. Neef,M., Ledermann,M., Saegesser,H., Schneider,V., Widmer,N., Decosterd,L.A., Rochat,B., and Reichen,J. 2006. Oral imatinib treatment reduces early fibrogenesis but does not prevent progression in the long term. *J. Hepatol.* **44**:167-175.

26. Friedman,S.L. 2003. Liver fibrosis -- from bench to bedside. *J. Hepatol.* **38 Suppl 1**:S38-S53.

27. Pinzani,M., Milani,S., Grappone,C., Weber,F.L., Gentilini,P., and Abboud,H.E. 1994. Expression of Platelet-Derived Growth Factor in a Model of Acute Liver Injury. *Hepatol* **19**:701-707.

28. Pinzani,M. 2002. PDGF and signal transduction in hepatic stellate cells. *Front Biosci.* **7**:d1720-d1726.

29. Iredale,J.P., Benyon,R.C., Pickering,J., McCullen,M., Northrop,M., Pawley,S., Hovell,C., and Arthur,M.J.P. 1998. `Mechanisms of spontaneous resolution of rat liver fibrosis - Hepatic stellate cell apoptosis and reduced hepatic expression of metalloproteinase inhibitors. *J. Clin. Invest.* **102**:538-549.

30. Greupink,R., Bakker,H.I., Reker-Smit,C., van Loenen-Weemaes,A.M., Kok,R.J., Meijer,D.K.F., Beljaars,L., and Poelstra,K. 2005. Studies on the targeted delivery of the antifibrogenic compound mycophenolic acid to the hepatic stellate cell. *J. Hepatol.* **43**:884-892.

31. Heldin,C.-H. 1997. Simultaneous induction of stimulatory and inhibitory signals by PDGF. *FEBS Lett.* **410**:17-21.

32. Shulman,T., Sauer,F.G., Jackman,R.M., Chang,C.N., and Landolfi,N.F. 1997. An antibody reactive with domain 4 of the platelet-derived growth factor beta receptor allows BB binding while inhibiting proliferation by impairing receptor dimerization. *J. Biol. Chem.* **272**:17400-17404.

33. Borkham-Kamphorst,E., Herrmann,J., Stoll,D., Treptau,J., Gressner,A.M., and Weiskirchen,R. 2004. Dominant-negative soluble PDGF-beta receptor inhibits hepatic stellate cell activation and attenuates liver fibrosis. *Lab Invest* **84**:766-777.

34. Olaso,E., and Friedman,S.L. 1998. Molecular regulation of hepatic fibrogenesis. *J. Hepatol.* **29**:836-847.

35. Yata,Y., Gotwals,P., Koteliansky,V., and Rockey,D.C. 2002. Dose-dependent inhibition of hepatic fibrosis in mice by a TGF-beta soluble receptor: implications for antifibrotic therapy. *Hepatology* **35**:1022-1030.

36. Stefanovic,B., Hellerbrand,C., Holcik,M., Briendl,M., Aliebhaber,S., and Brenner,D.A. 1997. Posttranscriptional regulation of collagen alpha1(I) mRNA in hepatic stellate cells. *Mol. Cell Biol.* **17**:5201-5209.

37. Beljaars,L., Olinga,P., Molema,G., De Bleser,P., Geerts,A., Groothuis,G.M.M., Meijer,D.K.F., and Poelstra,K. 2001. Characteristics of the hepatic stellate cell-selective carrier mannose 6-phosphate modified albumin ($M6P_{28}$-HSA). *Liver* **21**:320-328.

38. Kinnman,N., Hultcrantz,R., Barbu,V., Rey,C., Wendum,D., Poupon,R., and Housset,C. 2000. PDGF-mediated chemoattraction of hepatic stellate cells by bile duct segments in cholestatic liver injury. *Lab Invest* **80**:697-707.

39. Yoshiji,H., Kuriyama,S., Noguchi,R., Ikenaka,Y., Yoshii,J., Yanase,K., Namisaki,T., Kitade,M., Yamazaki,M., Asada,K. et al 2006. Amelioration of liver fibrogenesis by dual inhibition of PDGF and TGF-beta with a combination of imatinib mesylate and ACE inhibitor in rats. *Int. J. Mol. Med.* **17**:899-904.

In ancient times, Romans called the Galician coast in Spain along the northwestern tip of the Iberian Peninsula ***" Finisterrae"*** *(End of the Land), and in modern times this coastal area is known as* ***"Costa da Morte"*** *(The Dead Coast). Severe storms have destroyed many ships over the centuries.*

Costa da Morte, Finisterre, La Coruña
Galicia, España.